IEEE Access
Multidisciplinary | Rapid Review | Open Access Journal

Received December 12, 2019, accepted February 1, 2020, date of publication February 24, 2020, date of current version March 19, 2020.

Digital Object Identifier 10.1109/ACCESS.2020.2976010

Patient Specific Strategies to Enhance Leadless Pacemaker Lifetime in Synchronized Dual Chamber System

DEEPAK PALAKSHA, KIMMO KANSANEN, (Senior Member, IEEE), ZIGLIO FILIPPO, JACOB BERGSLAND, ILANGKO BALASINGHAM, (Senior Member, IEEE), AND DELPHINE FEUERSTEIN

Department of Electronic Systems, Norwegian University of Science and Technology, 7491 Trondheim, Norway
MicroPort CRM, 92140 Clamart, France.
Intervention Center, Oslo University Hospital, 0424 Oslo, Norway
BH Heart Center, 75000 Tuzla, Bosnia and Herzegovina

Corresponding author: Deepak Palaksha (deepakpalaksha22@gmail.com)

This work was supported by the European Union's H2020: MSCA: ITN program for the "Wireless In-body Environment Communication—WiBEC" Project under Grant 675353.

ABSTRACT Dual chamber leadless pacemakers are multi-unit, battery-driven implants utilized for treating patients with bradyarrhythmias and sino-atrial dysfunctions. Establishing synchronization between the units provides coordination between the atrium and ventricular contraction, and this mechanism depletes battery energy. Due to implant size constraints, reducing the synchronization energy consumed to enhance the lifetime of the implant is crucial. In this paper, a set of strategies are proposed and evaluated to indicate the best strategy to enhance the lifetime of atrial unit based on the patient's heart condition. Beat selective pulse transmission is employed instead of pulse transmission on every beat to reduce energy consumption. The characteristics of interbeat contraction timing of the atrium and ventricle from the patient data is modeled as time series. The designed model is extended to model synchronization strategies with sufficient synchronization accuracy and reduction in energy consumption. It is found that the implant lifetime is dependent on the natural atrial contraction probability, which is patient specific. A relation between the transmission duty-cycle and natural atrial contraction probability is derived for all the strategies, and this analysis is used in a case study to quantify the longevity. The proposed strategies show improved lifetime in comparison to the reference strategy. In the case study, for natural atrial contraction probability of 0.1, longevity is increased by two orders in relation to the reference strategy with the longevity of 4 years. However, there is no one best strategy; instead, the most energy-efficient strategy is determined from patient's natural atrial contraction probability and tolerance to suboptimal coordination.

INDEX TERMS Leadless pacemaker synchronization, improved atrial longevity, atrium and ventricle interbeat timing model, energy-efficient synchronization, interbeat time series equation.

I. INTRODUCTION

At the start of the cardiac cycle, heart relaxes and expands while receiving blood into both ventricles through both atria; The Sino-Atrial (SA) node releases electrical stimuli, this creates a wave of contraction in both atria, and each atrium pumps blood into the ventricle below it. Sinoatrial variability is the first level of randomness in the heart cycle. To ensure that the atria have ejected their blood into the ventricles, the atrioventricular node delays electrical impulses for a brief time (AV-delay) before reaching the ventricle; Consequently, the ventricles contract vigorously ejecting two-separated blood supplies from the heart one to the lungs and one to all other body organs. AV-delay establishes this precise coordination between atrial and ventricular contraction at AV node [1]. The AV-block is a condition that occurs at AV-node and adds to the randomness in the heart cycle. If the subject has an AV block, the electrical stimuli from atrium do not reach to the ventricle, and this would be fatal to the subject. Also, if the sino-atrial variability is not

The associate editor coordinating the review of this manuscript and approving it for publication was Hasan S. Mir.

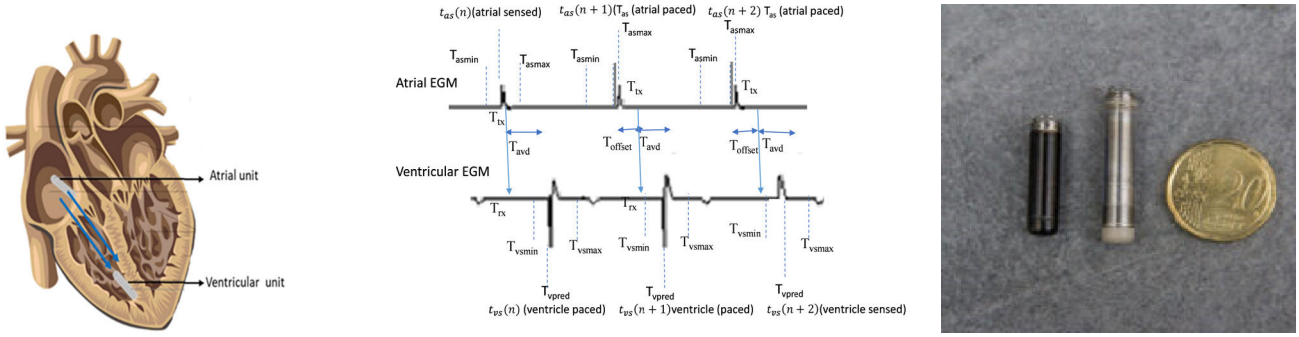

(a) (b) (c)

FIGURE 1. a) Dual Chamber Leadless Pacemaker system configuration with units implanted at right atrium and right ventricular unit. [10] b) The timing diagram of the synchronization mechanism. [10]The pulse transmission and reception used for synchronization is indicated by a lower head. The timing window at atrium and ventricle represented by dotted lines.c) Example size comparison (left to right) of the atrial and ventricular unit *Microport*.

followed by the ventricle, then there is a change in the heart rhythm affecting the volume of blood ejected, such a condition is called bradyarrhythmia [2], [3]. The stochastic model proposed addresses the randomness aspect associated with timing intervals of these pathologies as observed by units.

In the case of patients with bradyarrhythmia's, atrium and the ventricular chambers experience change in rhythm and are missing to contract at coordinated time instants. The dual-chamber leadless pacemaker systems are being utilized to regulate the rhythm, and it is available in different pacing configurations [4], [9], [13]. The pacing configuration has several pacing modes, but DDD mode is considered to mimic the heart best than other modes [21]. The DDD mode facilitates coordination between atrium and ventricular contraction, and is advised for patients with SA node dysfuntionality and transient AV block condition; therefore, in this study, DDD mode is considered as the mode of interest. The acronym DDD stands for sensing in dual chambers, pacing in dual chambers, and it has both inhibition and pacing functionality [5], [6]. In this paper, the term sensed is used to indicate the natural contraction of the heart, and the term paced is used to indicate the induced contraction by injecting a small electrical impulse through leads of pacemakers.

Leadless pacemakers are new devices in the medical domain replacing conventional pacemakers that were utilized to treat bradyarrhythmias; in this paper, for simplification, the atrial leadless pacemaker is referred to as atrial unit and ventricular leadless pacemaker as a ventricular unit (see Fig. 1a) [7]. The units have embedded electronics for pacing, sensing, and synchronization [8]. In this paper, the focus is on energy consumed for the synchronization mechanism.

In the dual chamber leadless pacemaker system, the atrial unit and the ventricular unit are placed, as shown in Fig. 1a [19]. If units operate independently, the uncoordinated pacing action by units at the atrium and ventricle will lead to change in the rhythm of heart, leading to device induced bradyarrhythmia conditions. Therefore, there is a need for synchronization between the units in order to achieve coordination between the atrium and ventricular contraction [9], [22]. However, synchronization mechanism consumes energy, and this affects the longevity of the units. Therefore, the focus of the paper is to reduce the energy consumed for the synchronization mechanism between the units as the implants have limited battery available.

A radio frequency (RF) pulse-based technique can be used to establish the synchronization between the units where the RF pulse is transmitted from atrial unit to ventricular unit on every heartbeat [9], [10]. The received RF pulse at ventricle unit provides the time reference to predict the time of ventricular contraction, this information is used to provide coordination between the chambers. In this paper, this strategy is considered as the reference strategy and is used to compare the energy efficiency with other proposed strategies. To perform pulse synchronization on every heartbeat consumes energy; therefore, the study employs selective pulse transmission rather than transmission over every beat. This reduces the energy consumed for synchronization at the atrial unit. The strategies for performing selective pulse transmission is an extension of modeled time series which models atrial interbeat probability distribution. There is a tradeoff between energy consumed and the degree of synchronization in each strategy; indicated by parameters, transmission duty cycle, and pacing error, respectively. The strategies are evaluated and compared based on these parameters. In addition, a relationship between the transmission duty cycle and atrial sensed event probability is derived, and the transmission duty cycle is studied for varying atrial sensed event probability. Note that atrial sensed event probability can also be described as natural atrial contraction probability. A case study is considered to quantify the difference in longevity with different proposed strategies. The work will allow physicians and researchers to determine the most energy efficient strategy, considering the longevity, and pacing error, based on the patient's atrial sensed event probability.

TABLE 1. Terminologies with its typical values.

Symbol	Quantity	Typical Values in ms
t_{as}	Random variable from an interbeat atrial probability distribution. N (T_{ae}, σ^2)	$N(800, 10)$
σ_a	The standard deviation of interatrial variability	100
T_{ae}	Atrial escape interval	800
T_{amax}	Limiting time before which atrium must be contracted	1050
σ	The standard deviation of interventricular variability	100
t_{asmin}	Minimum time window to expect the next atrial contraction	620
T_{avd}	atrial-ventricular delay time	120
t_v	Time of ventricular contraction	
T_{offset}	Offset time in atrial paced case	32
t_{opt}	Optimal pacing time instant at the ventricle	
T_{vmax}	Limiting time before which ventricle must be contracted	1250
Δt_{PE}	Pacing Error	

The analysis is performed on a fixed pacing rate configuration system, which indicates that the algorithm does not adapt to varying heart rate. The study excludes premature ventricular contraction episodes at ventricle and fibrillation at the atrium. The description of the performance metrics is provided in Section II. Section II also introduces a dual-chamber pacemaker system and its functional operation. In Section III, the interbeat time series of the atrium and the ventricle as observed by the implanted units are analyzed, and the model parameters are evaluated from the patient data by performing data fitting. In Section IV, different strategies are proposed to improve the energy efficiency of the system and thereby to improve the longevity of the atrial unit. In Section V, the proposed strategies are studied in relation to the reference robust strategy in terms of energy consumption and pacing accuracy. Section VI includes a case study considering an RF pulse transmitter where longevity comparison of different strategies is performed. Section VII is used to discuss and summarize the analysis.

II. OVERVIEW OF LEADLESS PACEMAKER SYSTEM

In this section, an overview of the dual chamber leadless pacemaker system is provided. The performance metric, and a potential RF pulse transceiver system that could be utilized for providing synchronization is described. The power consumption values from the RF transceiver system is used in the case study in section VI for quantifying the longevity in the strategies. The notations used in the article with its typical values are summarized in Table 1.

A. DUAL CHAMBER PACEMAKER SYSTEM (WIRELESS-DDD MODE)

In this study, a dual chamber leadless pacemaker system operating in DDD pacing mode is termed as wireless DDD mode [10]. This mode is most appropriate for patients with combined sinus node dysfunction and transient AV nodal dysfunction. In a nutshell, conventional DDD pacing mode possesses pacing and sensing capabilities in both the atrium and the ventricle, which is regulated by the pacemaker pulse generator unit. However, in wireless DDD mode, the regulation is supported by explicit pulse communication mechanism between the units [9], [10]. The proposed leadless pacemaker system has units implanted in the atrium and ventricle, as shown in Fig. 1a) There are two events at the atrium; atrial sensed and atrial paced denoted by AS and AP. The ventricle event is dependent on the timing of atrial events and AV blockage conditions. The AV blockage is denoted as B, and no blockage indicated as NB.

For implementing a wireless DDD pacing mode, the ventricle unit needs to know the time of atrial contraction (t_{as}). The time of atrial contraction is obtained by successful pulse detection at the receiver of ventricle unit, and this provides the time reference to predict the time of ventricular contraction (t_{vs}). The sequential steps performed to provide synchronization is described in the algorithm below (refer to Fig. 1b) [10].

i. The atrium and ventricle are sensed for contraction activity in the sensing window ranges [T_{asmin}, T_{amax}] and [T_{vsmin}, T_{vmax}] respectively. In particular, T_{amax} and T_{vmax} is the limiting time before which the contraction must occur on any beat in atrium and ventricle, respectively. The window size is constant and is updated for the next beat based on contraction time of the current beat.

ii. If the contraction is sensed at the atrium before T_{amax}, at that time instant an RF pulse is transmitted from the atrial unit to ventricle unit. If the contraction is not sensed, the atrium is paced, and an RF pulse is sent.

iii. The time of pulse transmission at atrial sensed and atrial paced events are given by,

$$t_{tx}[n] = \begin{cases} t_{as}[n]; & AS \\ t_{as}[n] + T_{offset}; & AP \end{cases}$$

where $t_{as}[n]$ is the time of atrial contraction and T_{offset} is an additional delay time used to compensate for the delay in conduction due to induced pacing. This is the extra time needed to sense the natural contraction of the ventricle in the AP case. In the case of AP, $t_{as}[n]$ is T_{amax}.

iv. At the receiver, RF pulse is received at the time denoted by t_{rx}, and it is approximately equal to the time of transmission t_{tx} as the propagation time is negligible.

$$t_{rx} \approx t_{tx}$$

v. The time reference to expect a spontaneous ventricular contraction at the receiver is evaluated as,

$$t_{vs}[n]\, t_{rx}[n] + T_{AVD}$$

where T_{AVD} is the AV-delay at AV-node, and it indicates the brief delay time that needs to be maintained

between the atrium and ventricular contraction, to provide coordination.

vi. If the spontaneous ventricular contraction is not sensed before $t_{vs}[n]$, then it indicates that the AV node is in B state and the ventricle unit paces the ventricle thereby maintaining the coordination.

vii. On the other hand, if the spontaneous ventricular contraction is sensed before $t_{vs}[n]$, then it indicates that the AV node is in NB state, and the ventricular pacing is inhibited.

viii. Therefore, the ventricle sensing and pacing depend on the atrial event time instants and AV block state. The cycle continues for the next beat maintaining the coordination between atrial and ventricular contractions.

The model supports fixed pacing rate configuration, which indicates that the AV-delay is maintained constant, in terms of heart functioning in this scenario, the atrium beat pattern is followed by the ventricle [4]. In systems responsive to adaptive heart rate (rate response systems), the atrial and the ventricular window ranges are changed with an increase or decrease in heart rate. The deviation can be handled by including adaptive observation window sizes and rate response algorithms, but it is beyond the scope of this paper [12].

B. PERFORMANCE METRICS

The transmitter duty cycle is the primary metric considered; it is defined as the fraction of time during which the transmission is active. The energy consumption is directly proportional to the transmitter duty cycle. The second performance metric employed is pacing error; it is defined as the deviation in the pacing time instant (t_{vs}) from the optimal pacing time at the ventricle. Optimal pacing time (t_{opt}) is the hypothetical time at which ventricle would have contracted for a healthy heart. It is the pacing time instant of the ventricle that is precisely coordinated with the atrial contraction by maintaining the AV-delay constant. The pacing error for the *nth* beat is given by Eq. (1).

$$t_{PE}\,(n) = t_{vs}\,(n) - t_{opt}\,(n) \tag{1}$$

The coordination provided can be optimal and non-optimal. The non-optimal case is when there is a non-zero pacing error; note that if regulated, the non-optimal case is non-fatal to the subject. This means that as long as the pacing error is not over the limit to induce conditions like bradyarrhythmia, non-optimal pacing could be tolerable.

C. TRANSCEIVER CIRCUIT

The communication between the atrial unit and the ventricular unit is provided by an RF transceiver circuit. The feasibility analysis of using an RF technology for providing synchronization has been verified in our previous work [10]. Load modulation and Human Body Communication (HBC) are the other possible technologies that could be used for providing synchronization [9], [13]. In this paper, a low power off-shelf RF transceiver circuit, which satisfies leadless pacemaker space constraint, operating in the ISM band 915MHz range is considered [14]. An OOK transmitter and an envelope detector receiver are used. The attenuation of the medium to the communication is a function of the frequency band used. The path loss in an implant to implant communication in the ISM band is described in [15]. For an inter unit distance of 50mm the pathloss is 56.03dB, and the attenuation increased with a slope of 3.7dB for every 10mm. The typical distance between the units is 50-70mm.

In this study, the focus is on transmitter longevity due to the constraint in implant size at the atrium. The atrial unit is relatively small when compared to the ventricular unit, as shown in the example Fig. 1c, the atrial unit is in black and the ventricular unit in silver. The difference in size is due to the location of the implant placement inside the heart. The ventricular unit is placed at the apex, which is a stable implant location (see Fig 1a); therefore, the unit can accommodate higher battery capacity.

The active power consumption by the transmitter circuit affects the longevity of the atrial unit. The leadless pacemaker Nanostim has an in-house battery of 220mAh [16]. Note that the pacemaker electronics consumes energy for sensing and pacing operations, but because the focus of the paper is to illustrate the change in active energy consumption of different synchronization strategies, the paper considers 40 percent of the in-house battery as the energy available for synchronization. i.e., 88mAh. The average power consumed (P_{TXavg}) is the product of the net duty cycle ($\overline{DC}$) and power consumed (P_{TX}). For the considered battery capacity, the longevity (L) in hours is calculated by Eq. (2), where V_{TX} is the output voltage. The longevity in years can be evaluated from the longevity in hours by dividing by the time scale 24^*30^*12. It is clear from the expression that longevity enhances with the reduction in the duty cycle.

$$\mathrm{L(h)} = \frac{88 V_{TX}}{P_{TX}\overline{DC}} \tag{2}$$

III. TIME SERIES MODEL OF ATRIUM AND VENTRICLE

The atrium starts the cardiac cycle, and its working depends on the Sino Atrial (SA) node. SA-node is hearts natural pacemaker and responsible for inter beat interval variability; it consists of a cluster of cells that are situated in the upper part of the wall of the right atrium [10]. In the first subsection, the atrium model analyzes the interbeat time interval to model the time series, statistical parameterization of time series describes atrium event behavior. The second part of the subsection involves similar analysis at ventricle. The model parameters evaluated from the dataset is used to generate the interbeat time series for further analysis.

A. DATA SET

The data is acquired from the subjects with sino-atrial node dysfunction and left bundle branch block, in the series of experiment conducted on CRT patients. The patients had no

AV block episodes. The EGM data is collected using ICD Programmer from the right atrial, right ventricular, and left ventricular leads. The current system utilizes just right atrial and right ventricular EGM data. The summary of patient data is given in Table 2. The right ventricular rhythm is coordinated with the atrium.

B. ATRIUM MODEL

The atrial interbeat timing variability is due to an inherent change in sinoatrial variability. In the literature, there are distributions like Gaussian mixture model, Gamma distribution, Erlang distribution to model the heart rate variation [18], [20], but for the given application the variability is modeled using Gaussian distribution. This is because the focus of the article is to model the atrial event probability distribution rather than the interbeat timing variability at atrium. The working operation at atrium is described from step1 - step3 in the algorithm1. For any nth beat, the time of atrial contraction $t_a\,(n)$, is given by the recursive equation (see Eq. (3)) and (4.1)–(4.7), as shown at the bottom of the next page. here $t_{as}\,(n)$ is the outcome for the nth beat from the atrial inter-beat probability distribution. The atrial interbeat probability distribution is as shown in Eq. (4.1-4.4). The variability in atrial contraction time for AS event is approximated to be a truncated Gaussian distribution (see Fig. 2), with mean T_{ae} the standard deviation σ_a in the interval $0 \leq t_{as} < T_{amax}$ (see Eq. (4.2)). In Eq. (4.2), the first term in the range represents the normalized truncated Gaussian function and the second term is used to scale the probability distribution function to 1. The atrial escape interval is denoted by T_{ae}, which gives the average time window between the atrial contractions. The standard normal distribution is denoted by $\emptyset\,(x)$, and Q(x) is the Q-function. For a fixed pacing rate system, the rate of the pacing is given by the inverse of the atrial escape interval ($1/T_{ae}$). The atrial unit paces at atrium (AP event) if the signal is not sensed before a limiting time T_{amax}, this is represented by an impulse function in the PDF at time instant T_{amax} (see Eq. (4.3) and Fig. 2). The Q function in the numerator is considered to scale the weight of the impulse function. The Q function here represent the area under the curve from T_{amax} to infinity (see Eq. (4.3)). The atrial pacing instant is represented to be an impulse function because, in reality, it is either an impulse function or a Gaussian distribution with a very small variance in the order of 10^{-5}. The right tail area under the curve of the Gaussian distribution gives the weight of the impulse. The interbeat timing observation cannot be less than zero; therefore, the left tail of Gaussian is truncated to zero (see Eq. (4.1)).

The data is a sample set of three patients with atrial interbeat interval summary, as shown in Table 1. The subjects considered have varying AS event probability. The probability decreases from patient 1 to patient 3. The idea is to consider all the possible subject condition to evaluate the model parameters.

The histogram of the atrial interbeat time series for all the patients is shown in Fig. 2. The AP probability from the data set (yellow bar) represents the number of AP events in relation to AS event for the patient. To perform data fitting the following steps are performed. The pacing probability (AP probability) from the data is set equal to the weight of the impulse function. A truncated Gaussian function (red curve) with the area under the curve equivalent to AS is used to fit the AS histogram data (blue bars). Similar data fitting is performed for other patient cases and is summarized in Table. 3. The parameters extracted are, mean T_{ae}, standard deviation σ_a, and limiting time for atrial sensing (T_{amax}).

TABLE 2. Subject data summary.

Subjects	# of beats	# of atrial sensed events	# of atrial paced events	Duration of recording in minutes
Patient 1	549	511	38	11.4
Patient 2	1093	819	272	23.2
Patient 3	1084	344	740	23.1

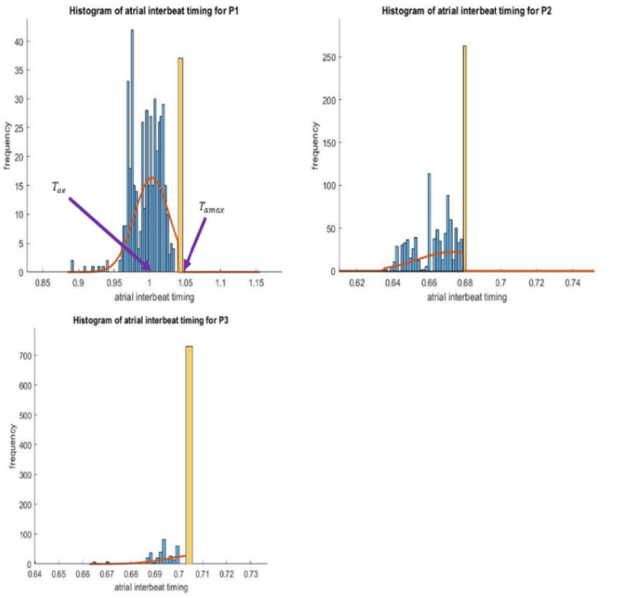

FIGURE 2. Histogram of atrial interbeat timing from three patients with varying AS and AP probability. The AS is indicated by blue bars and AP by yellow bars. The red curve is the truncated gaussian fit over AS interbeat timing data. The first and second patient (top left and top right) has higher AS episodes than AP, and in third patient the AP episodes are higher than AS.

TABLE 3. Atrial parameter evaluation from the patient data.

# of beats	Sensed events	Paced events	AS probability	AP probability	Gaussian fit mean (T_{ae})in ms	Gaussian fit SD (σ) in ms	T_{amax} in ms
549	456	93	0.84	0.16	998.1	24.4	1050
1093	819	272	0.75	0.25	673	19.5	680
1084	344	740	0.3	0.688	704.5	12.2	704

C. VENTRICULAR MODEL

The randomness at ventricle is due to atrial event time instants and AV blockage condition. In the first subsection,

the ventricular interbeat time series is modeled considering there is explicit pulse communication (with synchronization) between the atrium and ventricular units, and in the second subsection the effect of AV Block with no pulse communication (without synchronization) is analyzed.

1) With Synchronization Mechanism Between Units

In this case, the units are synchronized using a synchronization mechanism, as described in algorithm 1. The ventricular contraction time can be modeled as a time series, depending on the time of atrial contraction (t_{as}). The time series equations, as shown in Eq. (5) characterize the time of ventricular contraction at the nth beat. The ventricular contraction time follows the atrial contraction time after a brief delay time called AV-delay (T_{avd}). The AV-delay is in both the cases of Eq. (5) because AV-delay coordinates the atrium and ventricular contraction. The extra delay time T_{offset} is used in the AP case for the reason provided in algorithm 1.

$$t_{vs}[n] = \begin{cases} t_{as}[n] + T_{avd}; & AS \\ t_{as}[n] + T_{avd} + T_{offset}; & AP \end{cases} \tag{5}$$

2) WITHOUT THE SYNCHRONIZATION MECHANISM BETWEEN UNITS

The second case is when there is no synchronization mechanism between the units; in such cases, the coordination depends on AV blockage status. The status is binary, i.e., there is either an AV block or no AV block. In case of no AV block (B = 0), the ventricular interbeat contraction time interval $t_{vs}[n]$ is a time series dependent on atrial contraction time ($t_{as}[n]$) and is given by,

$$t_{vs}[n] = \begin{cases} t_{as}[n] + T_{avd}; & AS \\ t_{as}[n] + T_{avd} + T_{offset}; & AP \end{cases} \tag{6}$$

The equations are similar to the case where units have a synchronization mechanism (Eq. (5)). This indicates that when there is no AV Block or if units are synchronized, the system imitates the healthy cardiac cycle.

The conditional probability distribution for the ventricular contraction time $t_{vs}(n)$, given there is no AV block is given by Eq. (7.1-7.5), as shown at the bottom of the next page (see Fig. 3). The PDF of ventricular interbeat timing is different

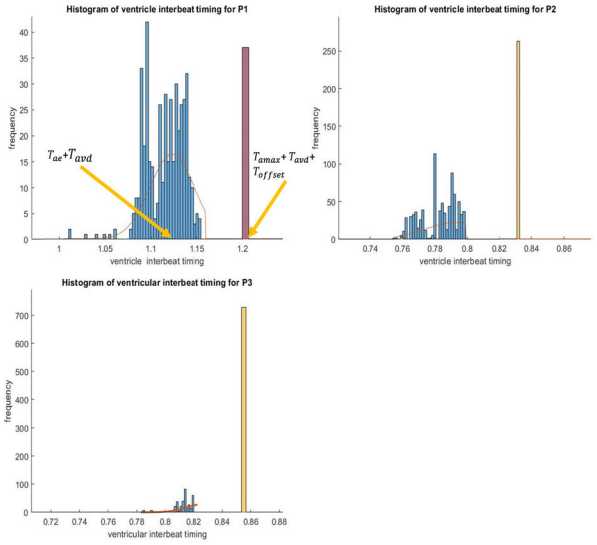

FIGURE 3. Histogram of ventricular interbeat timing from three patients with no AV Block. The red curve is the truncated gaussian fit over ventricular interbeat timing data with mean $T_{ae}+T_{avd}$. The blue bars and yellow bar represent the AS and AP event followed at ventricle. There are no VP episodes in this condition.

from an atrial interbeat timing by two parameters. The first one is shift in PDF by AVD delay (T_{avd}), therefore, T_{ae} is replaced by $T_{ae}+T_{avd}$ in Eq. (7.1-7.4). Also, offset time delay T_{offset} is added when paced (see Eq. (7.4)). The spontaneous ventricular contraction time is assumed to be Gaussian distributed with left tail truncated at 0 (see Eq. (7.1)); this is due to interbeat timing observation cannot be negative. The interval region $[0, T_{avd}+T_{amax})$ follows the atrial distribution with a mean of $T_{ae}+T_{avd}$ and a standard deviation of σ as shown in Eq. (7.2). Note that atrial and ventricular interbeat variability have the same standard deviation. The ventricle is paced at $T_{amax}+T_{avd}+T_{offset}$ if the ventricle does not contract naturally, it is indicated by an impulse function at $T_{amax}+T_{avd}+T_{offset}$ with weight equal to the right tail area under the curve of the Gaussian distribution (Eq. (7.4)).

The ventricular interbeat timing histogram from the subject's data set is plotted in Fig. 3. Similar to the atrium, parameters are evaluated from the data set for each patient from the truncated Gaussian fit, and simulation is performed. The parameters evaluated are given in Table 4.

$$t_a(n) = t_a(n-1) + t_{as}(n) \tag{3}$$

$$P(t_{as}) = \begin{cases} 0, & -\infty \le t_{as} < 0 \quad (4.1) \\ \dfrac{\emptyset\left(\frac{t_{as}-T_{ae}}{\sigma_a}\right)}{\sigma_a\left(Q\left(\frac{T_{amax}-T_{ae}}{\sigma_a}\right)\right)}\left(1-Q\left(\frac{T_{amax}-T_{ae}}{\sigma_a}\right)\right), & 0 \le t_{as} < T_{amax} \quad (4.2) \\ \dfrac{\delta(T_{amax})\,Q\left(\frac{T_{amax}-T_{ae}}{\sigma_a}\right)}{Q\left(\frac{-T_{ae}}{\sigma_a}\right)}, & t_{as} = T_{ae} + T_{amax} \quad (4.3) \\ 0, & t_{as} > T_{amax} \quad (4.4) \end{cases}$$

TABLE 4. Ventricle parameter evaluation from the patient data.

# of beats	Sensed events	Paced events	A.S probability	A.P probability	AV -B	Gaussian fit mean (T_{ae}+T_{avd})	Gaussian fit SD in ms	T_{amax} + T_{avd} + T_{offset} in ms
549	511	38	0.93	0.07	0	1118.1	24.4	1200
1093	819	272	0.935	0.065	0	793	19.5	832
1084	344	740	0.3	0.688	0	824.5	12.2	856

TABLE 5. Methods employed at ventricle to evaluate the ventricular contraction time for different cases.

α	Beat coordination is achieved utilizing explicit pulse synchronization
β	Beat coordination is achieved utilizing previous ventricular contraction time instant

When there is an AV-block (B = 1) the expected time of ventricular contraction at nth beat is calculated from the previous contraction time *n-1*, which is a first-order Markov chain sequence. As shown in Eq. (8), to the time of previous ventricular contraction time T_{vmax} is added. This is not the optimum pacing time (t_{opt}) for maintaining coordination because the ventricle unit does not coordinate with the time of atrial contraction, instead, it paces the ventricle in reference to a constant limiting time window. The optimum pacing time for providing maximum coordination between atrium and ventricle is in the case of no AV block (see Eq. (6)) or synchronized leadless pacemaker environment (see Eq. (5)).

$$t_{vs}[n] = t_{vs}[n-1] + T_{vmax} \tag{8}$$

here, T_{vmax} is the maximum limiting time allowed before

which ventricular contraction must be observed. Note that this is different from the coordinated ventricular contraction time. Here, the ventricular unit simply paces the ventricle at the time instant T_{vmax} on every beat, if the contraction is not observed.

Conditional PDF of ventricular contraction time $t_{vs}(n)$ when there is an AV block (*AV-B = 1*) is given by Eq. (9). The ventricular leadless pacemaker paces the ventricle at time instant T_{vmax}; this is represented by an impulse function at time instant T_{vmax}.

$$P(t_{vs}|B=1) = \begin{cases} \delta(T_{vmax}), & t_{vs} = T_{vmax} \\ 0, & otherwise \end{cases} \tag{9}$$

IV. STRATEGIES TO ENHANCE IMPLANT LIFETIME

The existing model facilitates coordination between atrium and ventricle by explicit pulse synchronization on every beat. It is evident that the power consumed by units is directly proportional to the pulse communication rate. In this section, the different strategies are modeled to improve the energy efficiency of the transmitter unit. The information processed at the ventricle in different strategies is summarized in Figure. 5a. In the figure, the arrowhead illustrates available state information in each strategy. For example, class A strategy has information on the AS, AV node-B, and AV node-NB condition. All the strategies other than the reference strategy have selective pulse transmission mechanism to lower the duty cycle. The strategies are compared with the reference strategy to quantify the change in performance metrics.

The two methods employed for evaluating the expected ventricular contraction time is listed in Table. 5.

A. REFERENCE STRATEGY

In this strategy, the duty cycle is one as there is an explicit pulse transmission on every heartbeat, implying the ventricle unit knows accurately the atrial contraction time on every beat. This information is used to provide optimal coordination between atrium and ventricle contraction. The reference strategy will be used as a baseline reference to compare other strategies in terms of energy consumption and pacing error performance.

The working operation of the reference strategy is given in the flowchart Fig.5b Gaussian random variable generator mimics the function of a Sino-Atrial node; if the random variable exceeds T_{amax}, it indicates that it is an AP event. A binary random variable generator replicates the effect of AV node condition. The time series model at atrium remains the same as in Eq. (3). At ventricle, the times series model follows Eq. (5), as there is pulse synchronization on every heartbeat. It is to note that the ventricle pacing time is optimal in Eq. (5)., thereby pacing error in the strategy is zero.

$$P(t_{vs}|B=0) = \begin{cases} 0, & -\infty \le t_{vs} < 0 \quad (7.1) \\ \left(\dfrac{\emptyset\left(\frac{t_{as}-T_{ae}-T_{avd}}{\sigma}\right)}{\sigma\left(Q\left(\frac{T_{amax}+T_{offset}-T_{ae}}{\sigma}\right)-Q\left(\frac{-T_{ae}-T_{avd}}{\sigma}\right)\right)}\right)\left(1-Q\left(\frac{T_{amax}}{\sigma}\right)\right), & 0 \le t_{vs} < T_{avd}+T_{amax} \quad (7.2) \\ 0, & T_{amax}+T_{avd} \le t_{vs} < T_{amax}+T_{avd}+T_{offset} \quad (7.3) \\ \dfrac{\delta(\tau_{amax}+T_{offset}+T_{avd})\,Q\left(\frac{T_{amax}}{\sigma}\right)}{Q\left(\frac{-T_{ae}-T_{avd}}{\sigma}\right)}, & t_{vs} = T_{amax}+T_{avd}+T_{offset} \quad (7.4) \\ 0 & t_{vs} > T_{amax}+T_{avd}+T_{offset} \quad (7.5) \end{cases}$$

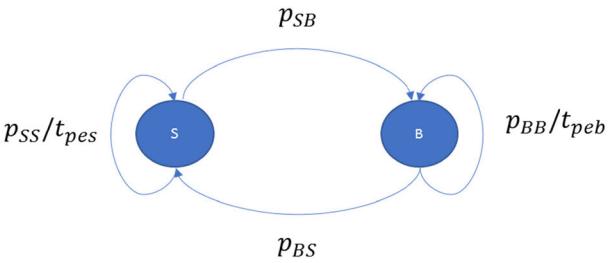

FIGURE 4. State space model to evaluate average pacing error in the AP event. S and B are the states associated with pacing error $\{t_{pes}, t_{peb}\}$ respectively. The transition probabilities are indicated with $P_{SS}, P_{BS}, P_{SB}, P_{BB}$.

B. CLASS A

In this class, the atrial unit transmits a synchronization pulse to the ventricular unit only when it senses the natural atrial contraction (see Eq. (10), AS case). On the other hand, in AP events, there is no pulse transmission, and the ventricle unit evaluates the expected ventricular contraction time from the previous ventricular contraction time instant (see Eq. (10), AP case). As explained in algorithm 1, in AP events, the expected ventricular contraction time must add T_{offset} factor for optimal coordination. In AS case, coordination is provided by pulse communication. The flowchart in the Fig. 5c summarizes the working operation. Note that, if there is no AV block (NB), then ventricle is naturally contracted (VS), and the pacing is inhibited. If there is AV block (B), then ventricle is paced at the time instants given in Eq. (10).

$$t_{vs}[n] = \begin{cases} t_{as}[n] + T_{avd}; & AS \\ t_{vs}[n-1] + T_{amax} + T_{offset}; & AP \end{cases} \tag{10}$$

The key idea of the strategy is to reduce the pulse transmission to just AS events, thereby conserving energy by not transmitting pulse in AP events. However, if the pacing error in AP event exceeds the limiting timing window before which ventricle must be contracted ($t_{PE} > T_{vmax}$) then the pulse synchronization should be resumed at the next beat. Assuming that the atrium is in the AP event, the average pacing error performance is analyzed using a first-order Markov chain. The average pacing error is of interest in AV-B state rather than in AV-NB state, as in NB state, there is a natural ventricular contraction.

The state space model is illustrated in Fig. 4, state B indicates the AV-block condition in AP event, and S indicates pulse synchronization state. The state transition matrix and associated pacing error for the Markov chain is given by Eq. (11) and Eq. (12) respectively. The steady state or stationary state occupancy vector is given by Eq. (13). The average pacing error is given by the product of steady-state occupancy and average pacing error associated with the state, as shown in Eq. (14).

$$P = \begin{bmatrix} p_{SS} & p_{SB} \\ p_{BS} & p_{BB} \end{bmatrix} \tag{11}$$

$$t_{PE} = \begin{bmatrix} t_{pes} & t_{peb} \end{bmatrix} \tag{12}$$

$$[\pi_S \pi_B] = \begin{bmatrix} \frac{1-p_{BB}}{2-p_{SS}-p_{BB}} & \frac{1-p_{SS}}{2-p_{SS}-p_{BB}} \end{bmatrix} \tag{13}$$

$$E(t_{PE}) = \pi_S E(t_{pes}) + \pi_B E(t_{peb}) \tag{14}$$

In this class, the average pacing error is zero as the optimum ventricular pacing time (t_{opt}) and the ventricular pacing time (t_{vs}) are the same. The pulse synchronization provides optimal coordination in the state S, therefore, t_{pes} is equal to zero. In the B state, ventricular pacing time instant ($t_{vs}(n)$) can be accurately evaluated from the previous ventricular pacing time instant ($t_{vs}(n-1)$), therefore t_{peb} is equal to zero.

The duty cycle is directly proportional to the probability of the AS event probability (see Eq. (15)). If the subject is prone to more AP events, then the model conserves energy by reduced pulse transmissions.

$$\mathrm{DC} = p_{AS} \tag{15}$$

C. CLASS B

In this class, the synchronization is achieved by transmitting the pulse from atrial unit to ventricular unit at AP events, and in AS events, there is no pulse transmission. If the ventricle unit does not receive the pulse at $T_{amax} + T_{offset}$, it indicates that the atrium is sensed, and the ventricle unit must evaluate when the ventricle must be paced from the previous ventricular contraction time (see Eq. (16)), the working operation is summarized in the flowchart Fig. 5d.

$$t_{vs}[n] = \begin{cases} t_{as}[n] + T_{avd} + T_{offset}; & AP \\ t_{vs}[n-1] + T_{amax} + T_{avd}; & AS \end{cases} \tag{16}$$

Assuming that the atrium is in the AS event, similar state-space model mentioned in Fig. 4 is considered to evaluate the average pacing error for varying AS probability. The state transition matrix is similar to Eq. (11), except that in this class, p_{BB} is equal to zero and p_{BS} is equal to one. This is because class B allows for one blocked state with sub optimal pacing, and then resumes pulse synchronization, the reason for assigning those probability values is explained in the subsection. The steady state occupancy vector for given state transition matrix in class B is given by Eq. (17). Similar to class A, due to explicit pulse synchronization, the average pacing error in S state (t_{pes}) is zero, however, since the class cannot account for the interatrial variability, in B state, the pacing is not optimal. The pacing error in B state at any step k ($t_{peb}(k)$) is as shown in Eq. (18). It is defined as the difference between the atrial pacing limiting time ($T_{amax}(k)$) and a random observation from the interatrial timing distribution in the interval $0 \leq t_{as} < T_{amax}$ (see Eq. (4). If the given typical values in Table 1 is considered, the average pacing error for the blocked state (t_{peb}) from the pacing error distribution is found to be around 0.245s. This is approximately 2.5 times the standard deviation of the truncated Gaussian distribution. The steady state occupancy probabilities considering the transition matrix of class B is as shown in Eq. (16). The average pacing error in class B follows Eq. (14) and is given by Eq. (19).

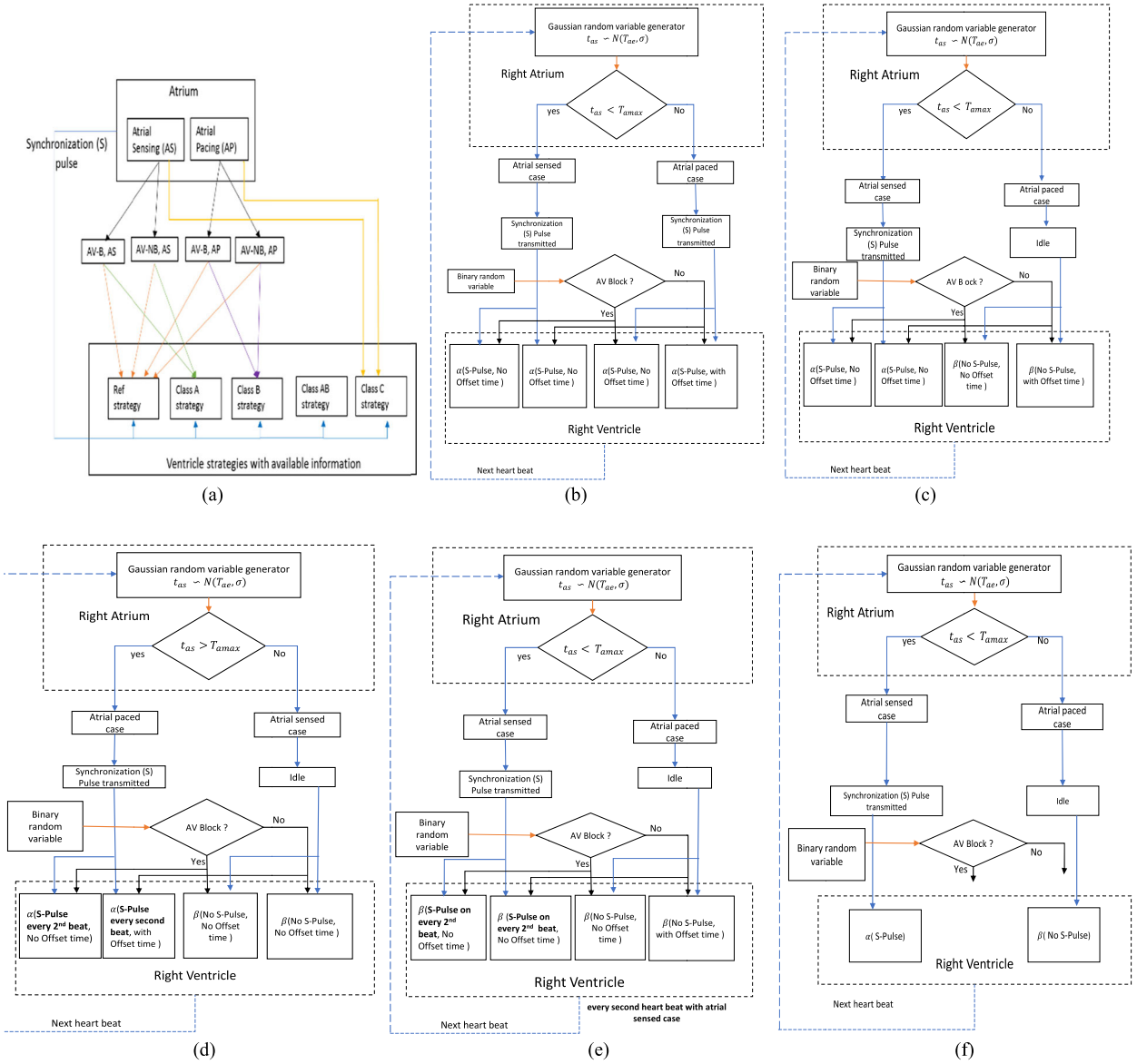

FIGURE 5. a) Summary of state space configuration for each strategy at ventricle. The arrowhead indicates the information available for each strategy.b) Operational flowchart of Reference strategy c) Class A d) Class B e) Class AB f) Class C.

The pacing error occurred on each beat in class B has an upper bound given by Eq. (20). It is the difference between the maximum and minimum time at which atrium contraction could be sensed. For the typical values considered, it is around 430ms.

$$[\pi_S \pi_B] = \left[\frac{1}{2 - p_{SS}} \quad \frac{1 - p_{SS}}{2 - p_{SS}} \right] \tag{17}$$

$$t_{peb}(k) = T_{amax}(k) - x, \forall x \in P(t_{as}); 0 \leq t_{as} < T_{amax} \tag{18}$$

$$E(t_{PE}) = \pi_B E(t_{peb}) \tag{19}$$

$$\lceil t_{PE}(k) \rceil \leq (T_{amax}(k) - T_{asmin}(k)) \tag{20}$$

The ventricular unit in prior has a copy of the atrial interbeat timing distribution (see Eq. (4)), which is termed uncertainty distribution window with mean $T_{ae} + T_{avd}$ and standard deviation σ_a. It is abbreviated as UDW and facilitates ventricular unit to evaluate the time instant T_{amax}. The size of UDW scales up for the second AS, B beat as the ventricle unit lacks information about atrial contraction time instants. Further analysis in the next subsection is performed for AS state as AP state utilizes pulse synchronization.

The duty cycle in class B is dependent on the evaluation of UDW size; for the first beat, it is given by $T_{amax} - T_{asmin}$. Assuming that the first beat is in B state, then the ventricle unit has a UDW size shorter than the limiting pacing time at the ventricle (T_{vmax}) (see Fig. 6). However, for the second B beat, the UDW size is scaled up by two; then the right tail of the window exceeds the limiting pacing time of

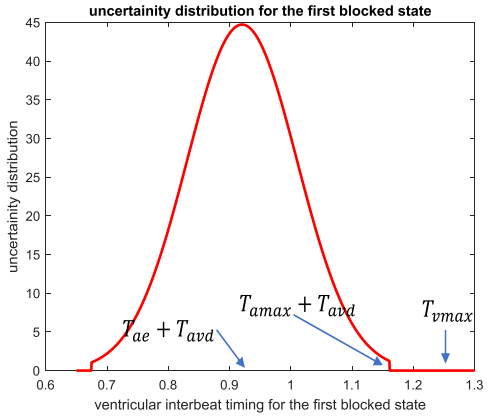

FIGURE 6. The uncertainty distribution window of first blocked beat in an AS state with window size less than limiting pacing time at ventricle.

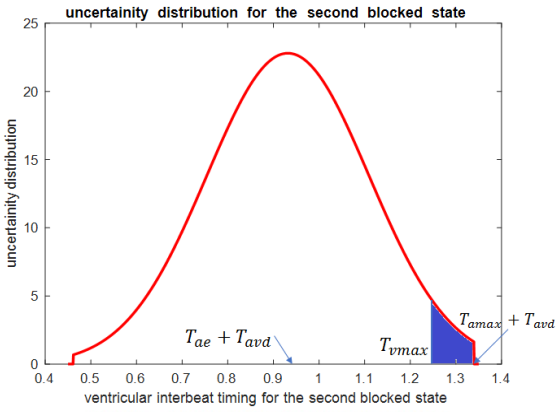

FIGURE 7. The uncertainty distribution window of second blocked beat in an AS state with window size exceeding limiting pacing time at ventricle.

the ventricle, as shown in Fig. 7 (blue region). The UDW exceeding T_{vmax} implies that there could be some beats expecting to pace the ventricle over the limiting time, and this would fail to maintain the coordination between atrium and ventricle. For example, if the typical values mentioned in Table. 1 is considered, and if the first beat is in B state, then the UDW size is 430ms with mean of 920ms; For the second blocked beat, UDW size is 860ms, with the mean of 920ms (see Fig.7). The truncated right tail time instant of UDW for the second blocked beat is 1330ms; this would exceed the maximum allowed ventricular pacing time of 1250ms. This implies that pulse synchronization should occur every second beat if it encounters two consecutive B events; this is shown in the duty cycle expression Eq. (21). There could be cases where pulse synchronization could be resumed on every third beat with change in typical values considered. In that case, the right tail of UDW would not exceed T_{vmax} in the second beat. However, resuming pulse synchronization on every second blocked beat in AS state guarantees pacing error not exceeding the limit.

$$\mathrm{DC} = \frac{p_{AS}}{2} + (1 - p_{AS}) = 1 - \frac{p_{AS}}{2} \tag{21}$$

D. CLASS AB

In this class, as the name suggests, the working operation includes the functionality of class A and class B. The working operation flowchart is shown in Fig. 5e. In AS event, the class follows class B strategy, i.e., to send synchronization pulse every second beat. In the AP case, it follows class A strategy where the expected current ventricular pacing time instant is evaluated accurately from the previous ventricular contraction time. The explicit pulse synchronization on every second beat in the AS event is due to an increase in the span of the UDW above the allowed limit. The reasoning follows class B. The class decreases the duty cycle further by half when compared to class A, as shown in Eq. (22). The reduction in duty cycle is associated with a sacrifice of optimal coordination. The average pacing error and the upper bound to pacing error is similar to class B (see Eq. (19) and Eq. (20)).

$$\mathrm{DC} = \frac{p_{AS}}{2} \tag{22}$$

E. CLASS C

In class C, the strategy addresses the duty cycle mainly by reducing one of the random variables. In this class, the ventricle considers just the atrium events and drops the AV node Block events. The working operation is summarized in Fig. 5f. The pulse transmission pattern majorly imitates class A strategy except for selective pulse transmission in AP events. The strategic advantage is that it scales down the model computation complexity as model addresses just atrial randomness. This implies the offset time (T_{offset}) regulated on every beat is lost. The AV Block condition becomes redundant in the AS event as there is explicit pulse synchronization. However, on the other hand, in the AP event, there is a deviation from the optimal pacing time. The pacing error is significant, and for the current beat the pacing error is given by T_{offset}. The upper bound for pacing error before which pulse synchronization needs to be resumed is dependent on the cumulative function of T_{offset}. The typical value of T_{offset} is 32ms and limiting time at ventricle before it must be paced is 200ms ($T_{vmax} - T_{amax}$). This implies a sequence of m beats would not need pulse synchronization, i.e., until the pacing error exceeds the limit ($\Delta t_{PE} > T_{vmax}$). For the values mentioned in Table 1, the class needs an explicit pulse synchronization every 6^{th} beat. The duty cycle and pacing error bound for class C is given by Eq. (23) and Eq. (24).

$$\begin{aligned} \mathrm{DC} &= p_{AS} + \frac{(1 - p_{AS})}{6} \\ &= \frac{1}{6} + \frac{5P_{as}}{6} \end{aligned} \tag{23}$$

$$\Delta t_{PE}(n) \leq \sum\nolimits_{m} T_{offset}(m) \tag{24}$$

V. STRATEGY PERFORMANCE COMPARISION

The energy consumed for synchronization of units influences the longevity of the devices. In the current energy

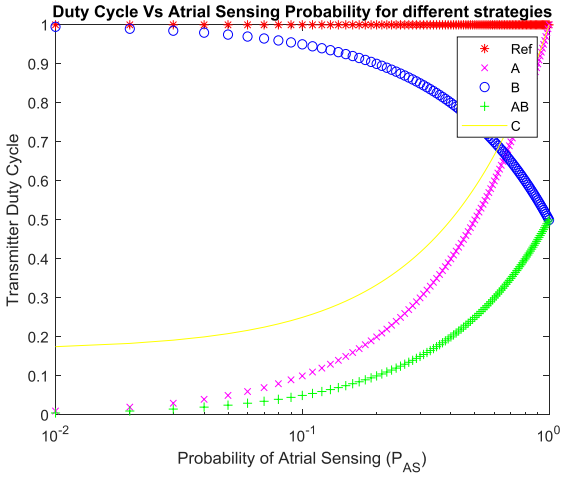

FIGURE 8. Transmitter duty cycle Vs. atrial sensed probabilities for different strategies.

budget of the units, the synchronization mechanism adds overhead in energy consumption to the existing functionality. Thereby scaling down synchronization rate will improve the unit longevity. In the current study, atrial unit longevity is considered for the reasons explained in section II; subsection D. Strategies are compared with performance metrics duty-cycle and pacing error. The expression for duty-cycle in terms of atrial sensed probability and pacing error is summarized for each strategy, as shown in Table 6. The reference robust case performance acts as the baseline strategy to compare the duty cycle and pacing error. The duty cycle is plotted for different AS event probabilities for every strategy, as shown in Fig. 8. The reference strategy has a duty-cycle equal to 1 for all the probabilities. The plot illustrates duty-cycle dominance by class A and class AB in lower AS probabilities indicating lower pulse synchronization rate. Class B has the edge over other classes in case of higher AS probabilities, and class C follows class A with a small deviation. From the clinical studies, mostly the subjects who are recommended pacemaker are with weak hearts; this implies that the subjects generally have lower AS probabilities.

The pacing error and duty-cycle are interrelated for a given AS probability. For an AS probability equal to 0.2, the relation for each class is illustrated in Fig. 9. It is seen that class A offers zero pacing error because of the model design taking advantage of the stochastic behavior of atrium and ventricle. Class B and class AB introduce similar pacing error for scaling down of the duty-cycle, and class C has better pacing error performance in relation to class B and class AB.

VI. CASE STUDY

In this section, the RF transceiver introduced in the background section is considered for quantifying the change in longevity between different classes. An OOK transmitter consumes 54mW (P_{TX}) for a peak output power of 13dBm from a 2.1V source. The designed envelope detector receiver has a sensitivity of -112dBm with 5.7mW (P_{RX}) power consumption. The pathloss experienced for an inbody to inbody

TABLE 6. Comparison of strategy in terms of duty cycle and pacing error bound.

Strategy	Duty Cycle (DC)	Pacing Error Bound (PE)
Reference Robust Strategy	1	0
Class A	P_{as}	0
Class B	$1-\frac{P_{as}}{2}$	$\leq (T_{amax}(n) - T_{asmin}(n))$
Class AB	$\frac{P_{as}}{2}$	$\leq (T_{amax}(n) - T_{asmin}(n))$
Class C	$\frac{1}{6}+\frac{5P_{as}}{6}$	$\sum_m T_{offset}(m)$

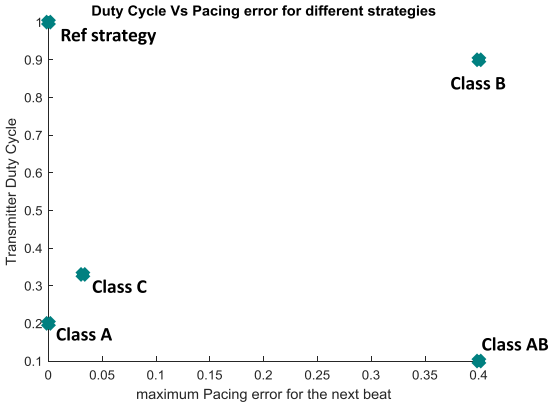

FIGURE 9. Duty cycle Vs. Maximum pacing error for the AS probability of 0.2 for different strategies.

communication in the ISM band is described in [15]. The reference path loss for an inter-unit distance of 50mm is 56.30dB, and the attenuation increases with a slope of 3.7dB for every 10mm. For the receiver design sensitivity of -112dBm, the inter leadless pacemaker distances less than 180mm can support successful detection for an error probability of 10^{-3}. The typical inter leadless pacemaker distance is around 60mm.

The study is limited to transmitter unit longevity. The longevity of the device is related to the duty cycle, and duty cycle consecutively is related to synchronization pulse-width (T_s). The pulse-width for the application is 0.1ms, and therefore the symbol rate is ($R_s = 1/T_s$) 10Kbps. The net duty-cycle ($\overline{DC}$) is the product of duty-cycle expression (Table. 6) and the pulse width. The longevity is calculated using Eq. 2.

Transmitter longevity in months is plotted against different AS probabilities and is as shown in Fig.10. Also, considering the typical values in Table. 1, the average pacing error for varying AS probabilities is illustrated in Fig.11. For better understanding, longevity in years and average pacing error is compared with the different strategies at two AS probability cases (see Table. 7). At the AS probability of 0.1, class AB and class A have the longevity of 48 and 70 years, respectively. Class A offers twelve times increase in longevity whereas in class AB, if the optimal coordination is

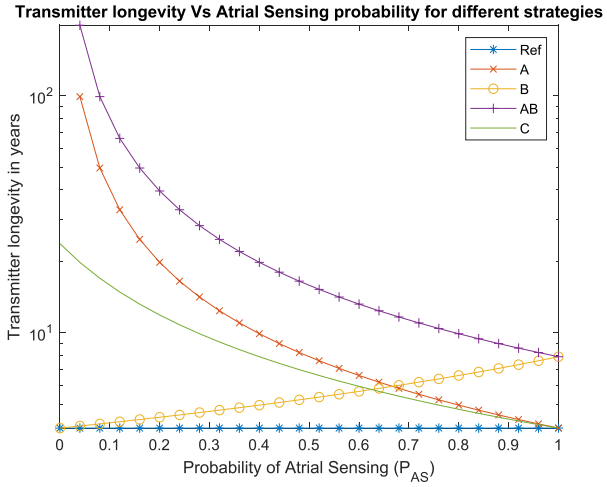

FIGURE 10. The plot of transmitter longevity for change in atrial sensed probability.

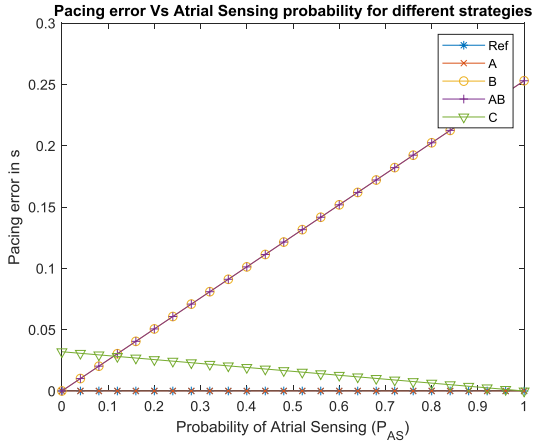

FIGURE 11. The plot of pacing error Vs. Change in atrial sense probability.

sacrificed with the average pacing error of 25.3ms, then longevity increases by seventeen times. The other strategies, like class C and class B, have higher longevity than reference strategy but still considerably small when compared to class A and class AB. The scenario changes entirely in an AS probability of 0.95. Class B and class AB have the edge over other classes with the longevity of 7.18 and 8.8 years, respectively. The dominance is accompanied by an induced pacing error of 232ms at the ventricle. For patients with zero tolerance to pacing error, class A is the best strategy for any AS probability, and for patients with tolerance to suboptimal pacing, class AB is the best strategy. All the proposed strategies have enhanced the life cycle of the atrial unit when compared to the reference strategy. However, the best strategy is dependent on the subject condition.

It is interesting to note that by knowing the condition of the heart. i.e., the AP actions needed for the subject over time, the physician can choose the best strategy. This can be known by having an ECG examination of the patient, and by finding

TABLE 7. Longevity in years and pacing error comparison of different strategies over as probability.

AS probability	Ref robust Strategy		Class A		Class B		Class AB		Class C	
	L	PE in ms	L	PE in ms	L	PE in ms	L	PE in ms	L	PE in ms
0.1	4	0	48	0	4.15	25.3	70	25.3	14.4	28.8
0.95	4	0	4.35	0	7.18	232	8.8	232	4.38	2.56

out the number of delayed beats encountered over a period which needs early pacing. One of the future studies would be to address the length of interbeat time intervals needed to generalize and decide the most energy-efficient strategy for the patient. Generally, in the case of young patients, they are likely to have less AP episodes, and older subjects need regular atrial pacing.

VII. SUMMARY AND DISCUSSION

In this paper, the statistical parameterization of atrial and ventricular interbeat time series is modeled into an event probability distribution, as observed by units. The model parameters evaluated from the subject data set is used to generate the interbeat time series of atrium and ventricle.

Also, an expression for duty-cycle as a function of AS event probability is derived for the proposed strategies (Table. 6). The analysis is similar but reversed if the AP event probability is considered. The proposed strategies showed improved longevity at the atrial unit in comparison to the reference strategy (Table 7). For example, with an AS probability of 0.1, the longevity in class A and class AB is two orders higher in relation to the reference strategy with the longevity of 4 years. This is a significant increase in implant longevity, where the additional energy conserved can be used for other pacemaker functionalities. The algorithms when implemented in implants could further be used to reduce implant battery size.

The next steps would be to improve the longevity of the ventricle unit by including smart receiver strategies. The longevity values are evaluated considering a potential RF transceiver system to quantify the change in energy consumption, but the proposed strategies could also be extended to other communication technologies like load modulation and human body communication (HBC). The next step in the study would be to implement the strategies in a microcontroller and perform in-vivo testing.

The analysis results provide insight for physicians and researchers about the most appropriate strategy for improving transmitter lifetime, thereby the atrial unit lifetime considering pacing error. If the subject has no tolerance for sub-optimal coordination between atrium and ventricle, class A strategy dominates. If the subject has tolerance for sub-optimal coordination, then class AB is promising for all the AS event probabilities. Class C is an intermediate strategy to improve longevity with lower pacing error when compared

to class AB and class B. Therefore, the best strategy is decided by patients AS event probability and tolerance to sub-optimal coordination.

ACKNOWLEDGMENT

We would like to thank the people in the department of Electronic System for valuable discussions. Deepak Palaksha also would like to thank in people the firm Microport for extending their support for patient data acquisition and valuable discussions.

REFERENCES

[1] H. Gray, K. Dawkins, J. Morgan, and I. A. Simpson, *Lecture Notes on Cardiology*. Boston, MA, USA: Blackwell Science, 2002.
[2] M. Haghjoo, "Bradyarrhythmias," in *Practical Cardiology*. 2018, pp. 261–268, doi: 10.1016/B978-0-323-51149-0.00015-8.
[3] J. Dretzke, "Dual chamber versus single chamber ventricular pacemakers for sick sinus syndrome and atrioventricular block," *Cochrane Database Systematic Rev.*, no. 2, 2004, Art. no. CD003710, doi: 10.1002/14651858.CD003710.pub2.
[4] P. J. Wang and D. L. Hayes, "Implantable pacemakers," in *Cardiac Electrophysiology*. 2014, pp. 1167–1177, doi: 10.1016/B978-1-4557-2856-5.00117-5.
[5] S. Furman and J. Gross, "Dual-chamber pacing and pacemakers," *Current Problems Cardiol.*, vol. 15, no. 3, pp. 122–179, Mar. 1990.
[6] D. N. Roger and A. Freedman. (2017). *Cardialogy Advisor—Modes of Cardiac Pacing: Nomenclature, Selection and Indications for Permanent Cardiac Pacing*. Accessed: 2019. [Online]. Available: https://www.thecardiologyadvisor.com/home/decision-support-in-medicine/cardiology/modes-of-cardiac-pacing-nomenclature-selection-and-indications-for-permanent-cardiac-pacing/
[7] J. Sperzel, H. Burri, D. Gras, F. V. Y. Tjong, R. E. Knops, G. Hindricks, C. Steinwender, and P. Defaye, "State of the art of leadless pacing," *Europace*, vol. 17, no. 10, pp. 1508–1513, Oct. 2015.
[8] D. Reynolds, "A leadless intracardiac transcatheter pacing system," *New England J. Cardiol.*, vol. 374, no. 6, pp. 533–541, 2016.
[9] L. Bereuter, "Leadless dual-chamber pacing: A novel communication method for wireless pacemaker synchronization," *JACC, Basic Transl. Sci.*, vol. 6, no. 6, pp. 813–823, 2018, doi: 10.1016/j.jacbts.2018.07.009.
[10] D. Palaksha, "Feasibility analysis for pulse based synchronization in a dual chamber leadless pacemaker system," in *Proc. Body Nets*, Oulu, Finland, 2018.
[11] L. S. Dreifus, D. Morse, Y. Watanabe, and D. Flores, "The advantages of demand over fixed-rate pacing: Report of clinical experience," *Diseases Chest*, vol. 54, no. 2, pp. 86–89, 1968.
[12] E. Pilat, R. Mlynarski, A. Wlodyka, and W. Kargul, "Influence of DDD rate response pacing with integrated double sensors on physical efficiency and quality of life," *Europace*, vol. 10, no. 10, pp. 1189–1194, Oct. 2008.
[13] D. Palaksha, G. Rizzo, R. Nocua, E. Lefeuvre, and K. Kansanen, "Load modulation for leadless pacemaker synchronization in a dual chamber pacemaker system," in *Proc. IEEE-EMBS Conf. Biomed. Eng. Sci. (IECBES)*, Dec. 2018, pp. 419–425.
[14] Marutha Electronics. *Murata Electronics TRC105*. Accessed: Jul. 7, 2019. [Online]. Available: https://www.digikey.no/product-detail/en/murata-electronics/TRC105/583-1159-2-ND/2179201
[15] P. Bose, A. Khaleghi, and I. Balasingham, "In-body and off-body channel modeling for future leadless cardiac pacemakers based on phantom and animal experiments," *IEEE Antennas Wireless Propag. Lett.*, vol. 17, no. 12, pp. 2484–2488, Dec. 2018.
[16] N. E.-C. M. Bhatia, "Leadless pacemakers: A contemporary review," *J. Geriatric Cardiol.*, vol. 15, no. 4, pp. 249–253, 2018.
[17] M. F. F. William and C. Shiel, Jr., (Dec. 27, 2018). *Medical Definition of SA Node*. Accessed: Apr. 28, 2019. [Online]. Available: https://www.medicinenet.com/script/main/art.asp?articlekey=5402
[18] T. Costa, G. Boccignone, and M. Ferraro, "Gaussian mixture model of heart rate variability," *PLoS ONE*, vol. 7, no. 5, 2012, Art. no. e37731.
[19] M. Albatat, J. Bergsland, H. Arevalo, H. H. Odland, P. Bose, P. S. Halvorsen, and I. Balasingham, "Technological and clinical challenges in lead placement for cardiac rhythm management devices," *Ann. Biomed. Eng.*, vol. 48, no. 1, pp. 26–46, Jan. 2020.
[20] A. M. Climent, F. Atienza, J. Millet, and M. S. Guillem, "Generation of realistic atrial to atrial interval series during atrial fibrillation," *Med. Biol. Eng. Comput.*, vol. 49, no. 11, pp. 1261–1268, Nov. 2011.
[21] D. Korpas, *Implantable Cardiac Devices Technology*. New York, NY, USA: Springer, 2013.
[22] K. M. Rabby, M. S. Alam, and M. S. T. S. A. Shawkat, "A priority based energy harvesting scheme for charging embedded sensor nodes in wireless body area networks," *PloS ONE*, vol. 14, no. 4, Art. no. e0214716, 2019.

DEEPAK PALAKSHA was born in Bengaluru, India. He received the B.E. degree in electronics and communication engineering from the Sapthagiri College of Engineering which is affiliated Visvesvaraya Technological University, in 2013, and the M.Sc. degree (Hons.) in computer and communication technology from Saarland University, Germany, in 2016. He is currently pursuing the Ph.D. degree with the Department of Signal Processing, Norwegian University of Science and Technology (NTNU). In 2016, he started his current research career as an early stage researcher in the WiBEC project, based in the host University NTNU.

KIMMO KANSANEN (Senior Member, IEEE) received the M.Sc. (EE) and Dr.Tech. degrees from the University of Oulu, Finland, in 1998 and 2005, respectively. He was a Research Scientist and a Project Manager with the Centre for Wireless Communications, University of Oulu. Since 2006, he has been with the Norwegian University of Science and Technology, Trondheim, Norway, where he is a Full Professor, since 2016. His research interests are within wireless communications and signal processing. He is an Associate Editor of the IEEE TRANSACTIONS ON WIRELESS COMMUNICATIONS.

ZIGLIO FILIPPO received the M.Sc. degree in biomedical engineering from the Politecnico of Milan, Italy, in 2006. Since 2006, he has been with the Sorin Group, MicroPort CRM, where he is currently a R&D System Leader for active cardiac implantable devices.

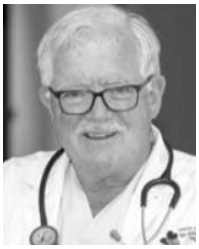

JACOB BERGSLAND received the degree in medical and the Ph.D. degree from Oslo University, in 1973 and 2011, respectively, and the M.D. degree. After internship in Norway, he moved to the USA for education in surgery. He was a Specialist in general surgery, in 1981, and cardiothoracic surgery, in 1983; the Director of cardiac surgery with the Buffalo VA Hospital, the Director of the Cardiac Transplantation Program, Buffalo General Hospital; the Director of the Center for Less Invasive Cardiac Surgery; a Clinical Associate Professor of surgery with The State University of New York at Buffalo; an Initiator of the hospital partnership between the Buffalo General Hospital and the Tuzla Medical Center, Bosnia, in 1995; and a Developer of cardiovascular surgery and cardiology at Bosnia and Herzegovina. He is currently a Researcher and a Co-Investigator with The Intervention Centre, Oslo University Hospital; The Medical Director of the BH Heart Centre, Tuzla BIH; and the Medical Director of Medical Device Company, Cardiomech AS.

ILANGKO BALASINGHAM (Senior Member, IEEE) received the M.Sc. and Ph.D. degrees in signal processing from the Department of Electronics and Telecommunications, Norwegian University of Science and Technology (NTNU), Trondheim, Norway, in 1993 and 1998, respectively. He performed the master's degree thesis with the Department of Electrical and Computer Engineering, University of California at Santa Barbara, Santa Barbara, CA, USA. From 1998 to 2002, he was a Research Engineer developing image and video streaming solutions for mobile handheld devices with the Fast Search and Transfer ASA, Oslo, Norway, which is now a part of Microsoft, Inc. Since 2002, he has been a Senior Research Scientist with the Intervention Center, Oslo University Hospital, Oslo, where he heads the Wireless Sensor Network Research Group. He was appointed as a Professor in signal processing in medical applications with NTNU, in 2006. From 2016 to 2017, he was a Professor by courtesy with the Frontier Institute, Nagoya Institute of Technology, Japan. He has authored or coauthored more than 200 journals and conference articles, seven book chapters, 42 abstracts, five patents, and 16 articles in popular press. His research interests include super robust short range communications for both inbody and onbody sensors, body area sensor network, microwave short range sensing of vital signs, short range localization and tracking mobile sensors, and nanoscale communication networks. He has given 16 invited/keynotes at the international conferences. In addition, he is active in organizing conferences (Steering Committee Member of ACM NANOCOM, from 2018 to 2021, the General Chair of the 2019 IEEE International Symposium of Medical ICT and the 2012 Body Area Networks Conference, and the TPC Chair of the 2015 ACM NANOCOM), and an Editorial Board [has been an Area Editor of *Nano Communication Networks* (Elsevier), since 2013].

DELPHINE FEUERSTEIN received the Ph.D. degree in bioengineering from Imperial College London, in 2009. She then moved to neurological research at the Max Planck Institute, Cologne as a Humboldt Fellow. She returned to France to join Microport, Sorin CRM, in 2013. She trained as a Multidisciplinary Engineer with Ecole Centrale Lyon, France. She is currently a Biomedical System Leader for innovative active medical devices.